The Journal of Physiology

Unmasking of oestrogen-dependent changes in left ventricular structure and function in aged female rats: a potential model for pre-heart failure with preserved ejection fraction

Moises Bustamante[1,2], Alejandra Garate-Carrillo[1,2], Bruce R. Ito[1], Ricardo Garcia[1,3], Nancy Carson[3] (iD), Guillermo Ceballos[2] (iD), Israel Ramirez-Sanchez[1,2], Jeffrey Omens[1] (iD) and Francisco Villarreal[1,4] (iD)

[1] *Department of Medicine, School of Medicine, University of California, San Diego, La Jolla, CA, USA*
[2] *Seccion de Estudios de Posgrado e Investigacion, Escuela Superior de Medicina, Instituto Politecnico Nacional, Mexico, DF*
[3] *Bristol-Myers Squibb, New York, NY, USA*
[4] *VA San Diego Health Care, San Diego, CA, USA*

Edited by: Don Bers & Beth Habecker

Key points

- Heart failure with preserved ejection fraction (HFpEF) is seen more frequently in older women; risk factors include age, hypertension and excess weight.
- No female animal models of early stage remodelling (pre-HFpEF) have examined the effects that the convergence of such factors have on cardiac structure and function.
- In this study, we demonstrate that ageing can lead to the development of mild chamber remodelling, diffuse fibrosis and loss of diastolic function.
- The loss of oestrogens further aggravates such changes by leading to a notable drop in cardiac output (while preserving normal ejection fraction) in the presence of diffuse fibrosis that is more predominant in endocardium and is accompanied by papillary fibrosis.
- Excess weight did not markedly aggravate such findings.
- This animal model recapitulates many of the features recognized in older, female HFpEF patients and thus, may serve to examine the effects of candidate therapeutic agents.

Abstract Two-thirds of patients with heart failure with preserved ejection fraction (HFpEF) are older women, and risk factors include hypertension and excess weight/obesity. Pathophysiological factors that drive early disease development (before heart failure ensues) remain obscure and female animal models are lacking. The study evaluated the intersecting roles of ageing, oestrogen depletion and excess weight on altering cardiac structure/function. Female, 18-month-old, Fischer F344 rats were divided into an aged group, aged + ovariectomy (OVX) and aged + ovariectomy + 10% fructose (OVF) in drinking water ($n = 8$–16/group) to induce weight gain.

Moises Bustamante is a second year PhD student from the National Polytechnic Institute based in Mexico City. He obtained a BS in Chemistry and an MS in Clinical Microbiology at the Autonomous University of Baja in Tijuana, Mexico. He is working in Dr Francisco Villarreal's Laboratory at UCSD focusing on research in heart failure with preserved ejection fraction and how ageing, oestrogen depletion and metabolic syndrome impact cardiovascular structure and function in the female sex. He is also evaluating the beneficial potential of the flavanol (−)-epicatechin on skeletal and cardiac muscle, brain and other metabolic disorders.

Left ventricular (LV) structure/function was monitored by echocardiography. At 22 months of age, animals were anaesthetized and catheter-based haemodynamics evaluated, followed by histological measures of chamber morphometry and collagen density. All aged animals developed hypertension. OVF animals increased body weight. Echocardiography only detected mild chamber remodelling with ageing while intraventricular pressure–volume loop analysis showed significant ($P < 0.05$) decreases *vs.* ageing in stroke volume (13% OVX and 15% for OVF), stroke work (34% and 52%) and cardiac output (29% and 27%), and increases in relaxation time (10% OVX) with preserved ejection fraction. Histology indicated papillary and interstitial fibrosis with ageing, which was higher in the endocardium of OVX and OVF groups. With ageing, ovariectomy leads to the loss of diastolic and global LV function while preserving ejection fraction. This model recapitulates many cardiovascular features present in HFpEF patients and may help understand the roles that ageing and oestrogen depletion play in early (pre-HFpEF) disease development.

Corresponding author F. Villarreal: UCSD School of Medicine, 9500 Gilman Drive BSB4028, La Jolla, CA 92093-0613J, USA.   Email: fvillarr@ucsd.edu

Introduction

Heart failure (HF) is the most common cause for hospitalization in older patients and represents the greatest cost for Medicare (Owan *et al.* 2006; Lam *et al.* 2011). Currently, up to 50% of HF patients are now recognized to have what is termed HF with preserved ejection fraction (HFpEF). This is a poorly understood disease and there are no therapies identified as clearly effective in mitigating its pathology (Omar *et al.* 2016; Barandiarán Aizpurua *et al.* 2019). Certain features such as the preservation of left ventricular (LV) geometry and ejection fraction (while at rest) in the setting of diastolic dysfunction are recognized as 'most common' in HFpEF patients (Omar *et al.* 2016). To better understand its pathophysiological underpinnings and the effects of 'preventive' therapies, animal models of pre-HFpEF would be desirable. HFpEF is more predominant in elderly, post-menopausal female patients (2:1) *vs.* men (Pacher *et al.* 2008; Lam *et al.* 2011) and the causes for this unequal distribution remain unclear. In women, the disease is also closely associated with the presence of hypertension as well as excess weight/obesity (Eaton *et al.* 2016). The development of pre-HFpEF animal models would thus require the convergence of 'risk' factors known to be associated with the disease while recapitulating features commonly seen with the pathology (Borlaug, 2016; Omar *et al.* 2016).

Systemic processes suspected to play a prominent role in the development of diastolic dysfunction with HFpEF include endothelial and mitochondrial dysfunction as well as oxidative stress (Borlaug, 2014), all of which have been associated with the presence of menopause in women, as well as with ageing (Takahashi & Johnson, 2015). However, very few female animal models have examined the impact that the loss of oestrogens has in the evolution of LV function, in particular, as low oestrogen levels interact with ageing, hypertension and/or excess weight before the onset of HF (Omar *et al.* 2016).

The Fischer F344 rat developed by NIH investigators has been extensively used as a model to study processes associated with ageing (Boluyt, 2004; Pacher *et al.* 2004). However, the great majority of published studies using rodent models of heart disease have used young, male animals with only an extremely limited number of studies focused on the female sex and the role of oestrogens (Conceição *et al.* 2016; Valero-Muñoz *et al.* 2017). While aged female rodents do not truly develop menopause, ovariectomy has been widely used and validated as a research tool to examine the role that oestrogen deprivation has on the control of multiple physiological systems (Sohrabji, 2005; Knowlton & Lee, 2012).

The main objective of this study was to develop and characterize a female rat model where ageing, oestrogen deprivation, hypertension and excess weight converge, with the intent to produce structural and functional changes that while not leading to HF, parallel those found in female HFpEF patients. To achieve this goal, older, female F344 rats undergoing ovariectomy and fructose supplementation were assessed for changes in LV structure and function, highlighting the changes associated with the presence of HFpEF in older, female patients.

Methods

Study design

Young (3-month-old) and aged (18-month-old) female Fischer F344 rats were used. Aged animals were obtained from the NIH/NIA ageing colony. Young animals were used as a reference control for all measurements. Animals were housed in pairs and maintained with a 12-h light–dark cycle with *ad libitum* intake of standard rat chow and sterilized tap water. Animal care and use

followed National Institutes of Health's *Guide for the Care and Use of Laboratory Animals* guidelines, and the Institutional Animal Care and Use Committee of the University of California San Diego School of Medicine approved the protocol for this study. Figure 1 summarizes the study design and protocol. Aged rats were acclimated to the environment for 1 week and then randomly assigned to three groups: aged ($n = 8$), ovariectomized (OVX, $n = 16$) and ovariectomy + 10% fructose in drinking water (OVF, $n = 16$). OVX animals underwent bilateral oophorectomy performed under isoflurane anaesthesia via a dorsal incision as previously described (Stout Steele & Bennett, 2011). OVF animals also had this surgery and were started on 10% fructose (w/v) in their drinking water 1 week after ovariectomy. Fructose intake was used to induce weight gain and replicate metabolic syndrome-like features known to be commonly present in female HFpEF patients. All aged animals were maintained under the same conditions for 3 months (to 21 months of age) with weekly measurement of body weight. At 21 months, all rats were subjected to a terminal study under isoflurane anaesthesia to measure *in vivo* LV haemodynamics, and *ex vivo* passive LV pressure–volume and epicardial strain–pressure curves. Young rats underwent the same terminal study after a 1 week period of acclimatization. Blood and select tissues including tibias were collected for further analysis.

Echocardiography

Closed-chest echocardiography was performed monthly for 3 months (between 18 and 21 months of age) in isoflurane-sedated animals using a GE Vivid 7 machine and an i12L probe (GE Healthcare, Milwaukee, WI, USA). Young rats were evaluated only once after the 1 week period of acclimatization. Measured parameters included anterior wall thickness in diastole and systole (AWThD/AWThS), posterior wall thickness in diastole and systole (PWThD/PWThS), LV internal diameter in diastole and systole (LVIDD/LVIDS), heart rate (HR), ejection fraction (EF) and fractional shortening (FS).

In vivo haemodynamics

At the terminal time point, animals were anaesthetized using 2.5% isoflurane, intubated and mechanically ventilated. To measure haemodynamics, a 2 French pressure transducer/conductance catheter (SPR-838 Millar Instruments; Houston, TX, USA) was introduced via the carotid artery into the aorta and LV. LV pressure and volume data were acquired at baseline and during temporary occlusion of the inferior vena cava at the level of the diaphragm to change LV filling. At the end of each experiment, parallel conductance was determined using an intravenous saline injection (Pacher *et al.* 2008). Measurements were recorded at a sampling rate of 1000 Hz using ADInstruments Powerlab (Colorado Springs, CO, USA) hardware and LabChart software. Parameters recorded included stroke work (SW), cardiac output (CO, ml min^{-1}), stroke volume (SV, μl), end-diastolic and end-systolic volumes (μl) and indexes, ejection fraction (EF, %), LV first derivative of pressure (dP/dt maximum and minimum), isovolumic relaxation time constant (Tau, ms) and systolic and diastolic aortic pressure (P_{ao}).

Ex vivo passive LV mechanics

After *in vivo* cardiac measurements were obtained, the heart was arrested with a slow infusion of 2 ml of a cardioplegia solution containing 0.03 M 2,3-butanedione monoxime and high potassium solution. The heart was rapidly excised and rinsed in sterile ice-cold saline, and remaining connective tissue was trimmed. The aorta was cannulated using a modified Langendorff system where it was perfused with the cold cardioplegia solution at 10–15 mmHg. A balloon was inserted into the LV from the left atrium and connected to a pressure transducer and an infusion pump as done previously (Omens *et al.* 1995).

To generate passive LV pressure–volume (PV) curves, the LV balloon was inflated at a constant rate of 200 μl min^{-1}. Pressure and infused volume data were acquired using DATAQ Software and Data Acquisition Systems (Akron, OH, USA) at a sampling rate of 10 Hz. Just prior to initiation of the infusion–deflation cycles, discrete epicardial markers were placed on the anterior LV epicardial surface. During a PV inflation–deflation cycle, synchronized video images were acquired using a ×250 digital USB microscope (Plugable Technologies, Redmond, WA, USA). The displacements of the epicardial markers were obtained during each infusion cycle to calculate two-dimensional circumferential (E_{11}) and longitudinal (E_{22}) strains relative to the long axis of the heart. Two to three preconditioning inflation runs
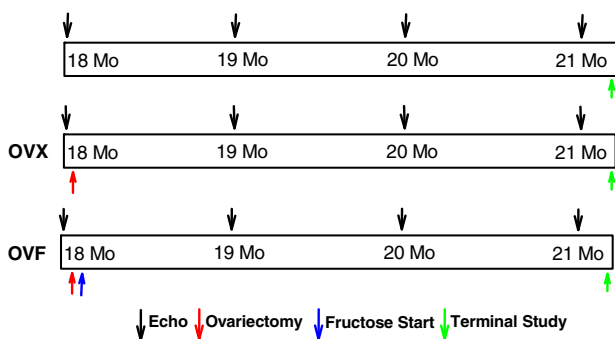
Figure 1. Scheme depicting the timeline of the study, measures and interventions used over the course of 3 months
[Colour figure can be viewed at wileyonlinelibrary.com]

were followed by two to three data acquisition runs with a maximal LV pressure of ~30 mmHg. Epicardial strains were calculated using customized strain software. Validation of these types of passive functional studies has been done previously (Omens *et al.* 1993).

Following these mechanical measures, hearts were perfusion fixed for 10 min using 10% formalin (EMD Millipore Corp., Billerica, MA, USA) introduced via the aortic cannula and with the LV balloon maintained at 10–15 mmHg. Fixed tissues were stored in conical tubes at a temperature of 4°C for 2 weeks until histological evaluation.

Histological analysis and collagen quantification

As shown in Fig. 2, formalin-fixed hearts were weighed and trimmed before sectioning at the midventricular region for subsequent embedding in paraffin. LV base and apical rings were then sectioned and mounted onto slides for Sirius Red staining and microscopic imaging. Using HALO® Digital Pathology Software (Indica Labs, Corrales, NM, USA) the analysis of the LV area and collagen positive area was performed by subdividing the LV ring into 18 discrete epicardial to endocardial wall sections. Of these regions, 12 were identified as free wall and six as septal. The ring sections of the LV were also digitally divided into inner half (subendocardium) and outer half (subepicardium) to allow comparison of endocardial *vs.* epicardial collagen distribution.

Statistical analysis

All data shown is presented as the mean ± standard error of the mean (SEM). Statistical analyses used are one-way or two-way ANOVA and Holm–Sidak's *post hoc* test and Student's unpaired *t* test as appropriate using SigmaPlot (Systat Software, 2008, San Jose, CA, USA). Results were considered statistically significant at a value of $P < 0.05$.

Results

General parameters

Total body weight and percentage body weight gain over time of aged, OVX and OVF rats are shown in Fig. 3*A* and *B*. Aged and OVX animals showed a 6% and 10% increase in weight respectively while the OVF group gained 26% ($P < 0.05$, OVF *vs.* OVX and aged). As shown in Table 1, there were no differences in heart weights between aged groups, but there was a difference between OVF *vs.* young ($P < 0.05$ by unpaired *t* test). Calculated body surface area was higher in OVF and OVX *vs.* aged ($P < 0.001$).

Echocardiography

Echocardiographic results are summarized in Table 1. As shown in Fig. 4*A–D*, results reveal a time-dependent effect on cardiac morphometry in aged, OVX and OVF groups. AWThD significantly decreased as a function of time with no differences between aged, OVX and OVF groups (Fig. 4*A*). In AWThS, there was a significant difference between aged *vs.* OVX and OVF ($P < 0.05$). For PWThD and PWThS there was also a decrease in thickness over time without difference between aged, OVX and OVF groups (Fig. 4*B*). While LVIDD and LVIDS demonstrated no differences between aged, OVX and OVF groups, there was a significant time dependent increase in chamber diameters (Fig. 4*C* and *D*). HR, EF and FS were also not different between aged, OVX and OVF groups. BW, AWThD and AWThS of aged, OVX and OVF were different *vs.* young ($P < 0.001$). LVIDD, LVIDS and PWThD of aged, OVX and OVF were significantly different *vs.* young ($P = 0.003$, $P = 0.014$ and $P = 0.002$, respectively).

Haemodynamic measurements

Results from *in vivo* haemodynamic measurements are summarized in Table 2 and selected data are shown in Fig. 5*A–C*. For systolic P_{ao}, there was a significant increase in aged groups *vs.* young ($P = 0.009$). Cardiac index was decreased in aged, OVX and OVF *vs.* young animals ($P < 0.05$) while OVX and OVF were different *vs.* aged ($P < 0.001$). Stroke volume index was reduced in aged, OVX and OVF *vs.* young ($P < 0.05$), and differences between OVX and OVF were also present *vs.* aged ($P < 0.001$) indicating an effect of ovariectomy and fructose on cardiac function. EF was stable and not different between groups, being preserved at the normal range of $\geq 50\%$ (Fig. 5*D*). Figure 6*A* and *B* depicts iso-volumic relaxation time constant (IVRT), also known as 'Tau', and arterial elastance (E_a), respectively, in the different groups. An increase in Tau was noted in aged, OVX and OVF groups *vs.* young ($P < 0.05$). Arterial elastance was significantly elevated in OVX and OVF *vs.* young ($P < 0.05$) with a trend from an increase in the aged group. The end-diastolic pressure–volume relationship (EDPVR) slope demonstrated differences between aged and OVX ($P < 0.05$).

Ex vivo LV mechanics

As shown in Fig. 7*A*, the analysis of LV PV curves did not demonstrate differences among the aged, OVX and OVF groups. However, all these groups were different *vs.* young ($P < 0.001$) demonstrating a global right-shift in aged, OVX and OVF animals. Epicardial circumferential strain analysis (Fig. 7*B*) revealed no differences in E_{11} between aged, OVX and OVF groups or when compared to young.

In longitudinal strain E_{22}, the maximal strain observed at 30 mmHg was ~0.04 (4%) and no differences were detected amongst all groups. Overall, E_{11} strains were higher than E_{22} for all groups, where the range for E_{11} was ~0.06–0.09 (i.e. 6–9%).

Histological analysis and collagen quantification

Representative Sirius Red-stained cross-sections of hearts from select animals of the different groups at low and high magnifications are shown in Fig. 8. Images similar to those shown in the panel were used to quantify collagen abundance in the LV by segments as outlined in Methods. Interestingly, a visual inspection of large areas of abnormal (patch like) fibrosis present in papillary muscles indicated that aged hearts showed such lesions in 1/4 aged animals (25%), 4/6 OVX (67%) and 5/7 OVF (71%) *vs.* none in young animals. Results from morphometry and histology are summarized in Fig. 9*A–F*. Aged rats demonstrated a higher LV tissue area *vs.* young ($P < 0.05$). Aged, OVX and OVF groups exhibited increased LV collagen area, percentage free wall, septal and total LV collagen *vs.* young ($P < 0.05$). Whereas the endocardial/epicardial ratio did not demonstrate significant overall differences by ANOVA among the groups, there were differences between OVX and OVF *vs.* young ($P < 0.05$, by unpaired *t* test).

Discussion

Findings from this study indicate that with ageing in female rats, a modest degree of LV remodelling is observed which is accompanied by the prolongation of relaxation time. With ovariectomy, these changes are compounded by significant reductions in stroke volume and CO in the setting of preserved EF. Ageing in this animal model also showed the development of diffuse myocardial fibrosis, which becomes greater in the endocardium
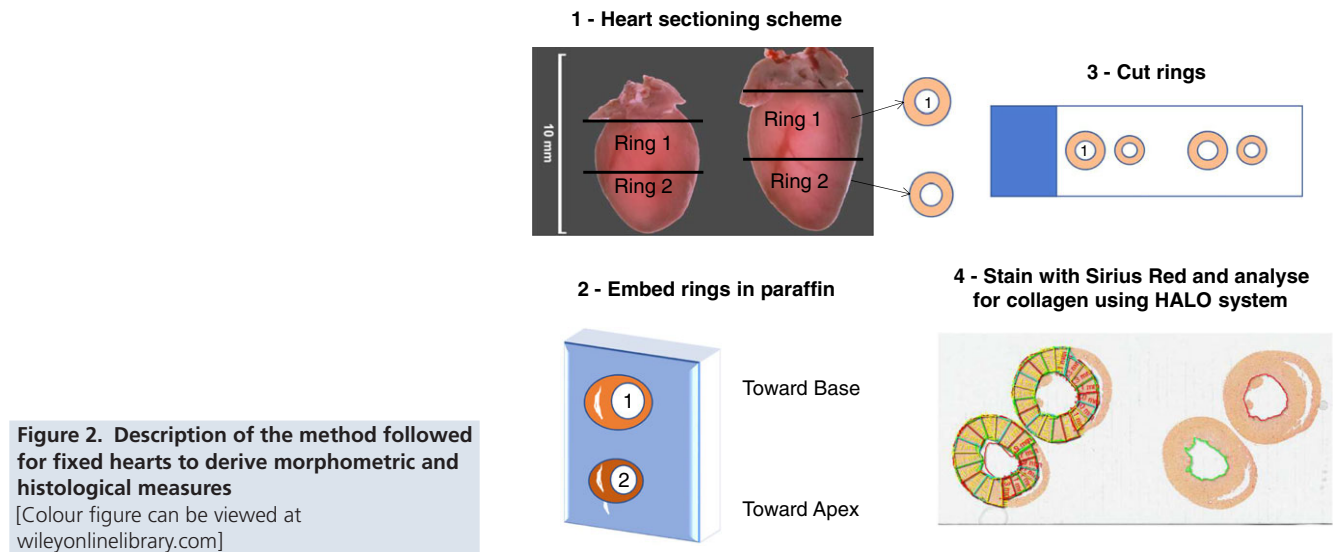
Figure 2. Description of the method followed for fixed hearts to derive morphometric and histological measures
[Colour figure can be viewed at wileyonlinelibrary.com]
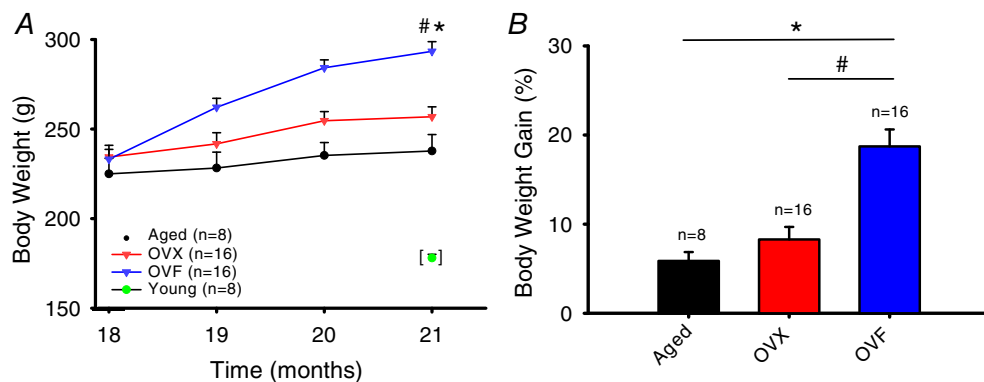
Figure 3. Changes in body weight observed in the different animal groups over 3 months
A, body weight gain in grams ($P < 0.001$, OVF *vs.* OVX and aged). *B*, body weight gain as a percentage of the initial weight ($P < 0.001$, OVF *vs.* OVX and aged). Young group single time-point data included as reference. Values are means ± SEM. OVF, ovariectomized + fructose; OVX, ovariectomized. [Colour figure can be viewed at wileyonlinelibrary.com]

Table 1. Body weight, heart weight and echocardiographic assessment of systolic and diastolic function of young and aged, ovariectomized (OVX) and ovariectomized + fructose (OVF) Fischer 344 female rats

| | | | | | | | P | | | |
| | | | | | | | Two-way ANOVA (aged, OVX and OVF) | | | One-way ANOVA (sacrifice) |
Parameter	Group	3 months	18 months	19 months	20 months	21 months	Group	Interval	Interaction	All group
BW (g)	Young	178 ± 2.07								<0.001
	Aged		225.00 ± 8.58	228.25 ± 8.84	235.25 ± 7.23	237.75 ± 9.15	<0.001	<0.001	<0.001	
	OVX		234.38 ± 6.54	241.75 ± 6.21	254.53 ± 5.09	256.88 ± 5.53				
	OVF		233.13 ± 5.53	262.13 ± 5.03	284.19 ± 4.43	293.38 ± 5.42				
HW (g)	Young	0.730 ± 0.032								0.300
	Aged					0.846 ± 0.054				
	OVX					0.896 ± 0.054				
	OVF					0.895 ± 0.037				
AWThD (mm)	Young	0.91 ± 0.006								<0.001
	Aged		1.09 ± 0.022	1.05 ± 0.023	1.03 ± 0.014	1.03 ± 0.020	0.809	<0.001	0.407	
	OVX		1.07 ± 0.013	1.07 ± 0.016	1.02 ± 0.009	1.01 ± 0.013				
	OVF		1.10 ± 0.017	1.08 ± 0.022	1.03 ± 0.014	1.01 ± 0.018				
AWThS (mm)	Young	1.20 ± 0.027								<0.001
	Aged		1.70 ± 0.074	1.55 ± 0.072	1.53 ± 0.030	1.51 ± 0.034	0.017	<0.001	0.044	
	OVX		1.51 ± 0.032	1.52 ± 0.043	1.43 ± 0.030	1.33 ± 0.021				
	OVF		1.47 ± 0.033	1.56 ± 0.047	1.44 ± 0.025	1.40 ± 0.031				
LVIDD (mm)	Young	6.74 ± 0.088								0.003
	Aged		6.65 ± 0.089	6.76 ± 0.133	6.80 ± 0.124	6.99 ± 0.110	0.205	<0.001	0.142	
	OVX		6.81 ± 0.110	6.87 ± 0.112	7.09 ± 0.084	7.32 ± 0.097				
	OVF		6.59 ± 0.091	6.85 ± 0.097	7.19 ± 0.109	7.20 ± 0.095				
LVIDS (mm)	Young	3.82 ± 0.065								0.014
	Aged		3.64 ± 0.079	4.00 ± 0.113	4.04 ± 0.128	4.06 ± 0.141	0.388	<0.001	0.275	
	OVX		3.74 ± 0.064	4.05 ± 0.123	4.25 ± 0.099	4.44 ± 0.154				
	OVF		3.61 ± 0.061	3.91 ± 0.114	4.25 ± 0.118	4.30 ± 0.108				
PWThD (mm)	Young	1.10 ± 0.028								0.002
	Aged		1.49 ± 0.030	1.44 ± 0.045	1.38 ± 0.027	1.44 ± 0.065	0.729	<0.001	0.483	
	OVX		1.46 ± 0.036	1.45 ± 0.038	1.35 ± 0.026	1.34 ± 0.047				
	OVF		1.52 ± 0.025	1.44 ± 0.042	1.35 ± 0.036	1.36 ± 0.051				
PWThS (mm)	Young	1.97 ± 0.280								0.216
	Aged		2.44 ± 0.035	2.33 ± 0.056	2.35 ± 0.041	2.41 ± 0.084	0.298	0.003	0.951	
	OVX		2.52 ± 0.044	2.37 ± 0.055	2.33 ± 0.038	2.36 ± 0.074				
	OVF		2.58 ± 0.041	2.43 ± 0.071	2.39 ± 0.057	2.45 ± 0.065				
HR (bpm)	Young	302.15 ± 10.972								0.199
	Aged		292.75 ± 9.100	307.88 ± 11.038	291.13 ± 14.111	311.50 ± 8.113	0.225	0.006	0.275	
	OVX		297.69 ± 5.702	335.38 ± 7.061	309.81 ± 8.930	302.38 ± 9.707				
	OVF		305.00 ± 7.484	323.13 ± 5.989	301.50 ± 11.431	326.56 ± 8.703				
EF (%)	Young	79.87 ± 0.429								0.109
	Aged		81.75 ± 0.701	77.00 ± 1.239	77.00 ± 1.180	78.25 ± 1.449	0.597	<0.001	0.295	
	OVX		81.56 ± 0.223	77.25 ± 1.039	76.44 ± 0.962	75.00 ± 1.497				
	OVF		81.75 ± 0.520	79.25 ± 1.135	77.00 ± 1.057	76.38 ± 1.197				
FS (%)	Young	43.33 ± 0.419								0.146
	Aged		45.38 ± 0.596	40.75 ± 1.146	40.75 ± 1.098	42.13 ± 1.302	0.548	<0.001	0.333	
	OVX		45.19 ± 0.277	41.00 ± 0.949	40.19 ± 0.823	39.38 ± 1.316				
	OVF		45.38 ± 0.523	42.94 ± 1.086	41.06 ± 0.994	40.50 ± 1.021				

Values are means ± SEM. AWThD, anterior wall thickness diastole; AWThS, anterior wall thickness systole; BW, body weight; EF, ejection fraction; FS, fractional shortening; HR, heart rate; HW, heart weight; LVIDD, left ventricle internal diameter diastole; LVIDS, left ventricle internal diameter systole; PWThD, posterior wall thickness diastole; PWThS, posterior wall thickness systole.

with ovariectomy, accompanied by a marked development of papillary fibrosis. The presence of modest chamber geometric remodelling, preservation of EF, prolongation of LV relaxation time, loss of CO and development of fibrosis recapitulates several of the features recognized in older, female HFpEF patients and suggests this model may be suitable to explore the role that risk factors play in early disease development and the effects of therapeutic interventions.

Multiple rodent models have been employed in an attempt to examine suspect pathophysiological events linked to the development of HFpEF (Conceição *et al.* 2016; Valero-Muñoz *et al.* 2017). While models commonly incorporate suspect aetiological factors such as pressure overload, obesity and diabetes, there is much less emphasis on the use of female or aged animals, thus incompletely replicating the prototypical human female HFpEF patient (Omar *et al.* 2016). Common findings using young, male rodents with aortic banding/or hypertension include LV hypertrophy, inflammation, fibrosis, stiffer end-diastolic pressure–volume relationships (EDPVR), and prolongation of relaxation with minimal changes in EF (Conceição *et al.* 2016; Valero-Muñoz *et al.* 2017). Diabetic models also demonstrate hypertrophy and interstitial fibrosis, while obese animals show decreases in the E/A ratio (i.e. impaired LV relaxation) (Valero-Muñoz *et al.* 2017). There are certainly relevant applications for these animal models, but they do not replicate the convergence of 'typical' factors found in ageing female patients that subsequently develop HFpEF.

Ageing models have used various rat strains (mostly male) to characterize changes in cardiac structure/function (Boluyt, 2004; Pacher et al. 2004, 2008; Valero-Muñoz *et al.* 2017). When using ∼2-year-old female Fischer 344 rats, ageing results in LV hypertrophy and diastolic dysfunction, while males from the same strain/age develop eccentric remodelling, mitral regurgitation, interstitial fibrosis and impaired systolic function (Forman *et al.* 1997). Hybrid Brown Norway–Fischer 344 rats (F344BN) have also been used to study the effects of ageing. Female rats of up to 30 months of age show development of LV hypertrophy, dilatation and diastolic dysfunction (Fannin *et al.* 2014), while decreases in collagen area fraction have been reported (Hacker, 2005). In our study, using echocardiography, we document the development of mild eccentric chamber remodelling from 18 to 21 months of age, with no apparent changes in diastolic or systolic function, including EF. However, direct catheter-based haemodynamics reveal with ageing hypertension, the prolongation of relaxation and a modest but significant reduction in CO while maintaining EF. Histology demonstrated an approximate doubling of collagen area fraction in the absence of chamber stiffening as revealed by *ex vivo* LV passive PV curves and epicardial strains. Therefore, the prolongation of relaxation is likely derived from impaired active LV relaxation, and not the direct effect of excess collagen and tissue stiffening at the levels measured here (∼5%). Thus, in aged female rats, there can be modest LV chamber remodelling, prolonged relaxation and interstitial fibrosis while maintaining normal EF.

The high prevalence of HFpEF in older women suggests a strong link between low oestrogen levels and the disease (Zhao *et al.* 2014). Interestingly, published studies suggest the development of greater levels of myocardial fibrosis in post-menopausal women *vs.* men (Barasch *et al.* 2009; Liu & Liu, 2014) with normal ageing or with HF. In rats, unlike menopausal women, oestradiol levels during ageing can be near their younger counterpart even past 20 months of age (Fannin *et al.* 2014). Thus, ovariectomy is commonly used to examine the role that low oestrogen levels play in altering cardiac structure/function (Knowlton & Lee, 2012). Unfortunately, only an extremely limited number of studies have used this approach. Using young male and female rats undergoing aortic banding (Douglas *et al.* 1998), a lesser degree of LV chamber remodelling, loss of function and fibrosis were noted in female animals. However, the protective role of oestrogens in rodent models of pressure overload is greatly diminished with ovariectomy (Bhuiyan *et al.* 2007). Stice *et al.* (2011) reported that ovariectomy in 20-month-old Norway Brown rats decreases LV fractional shortening from
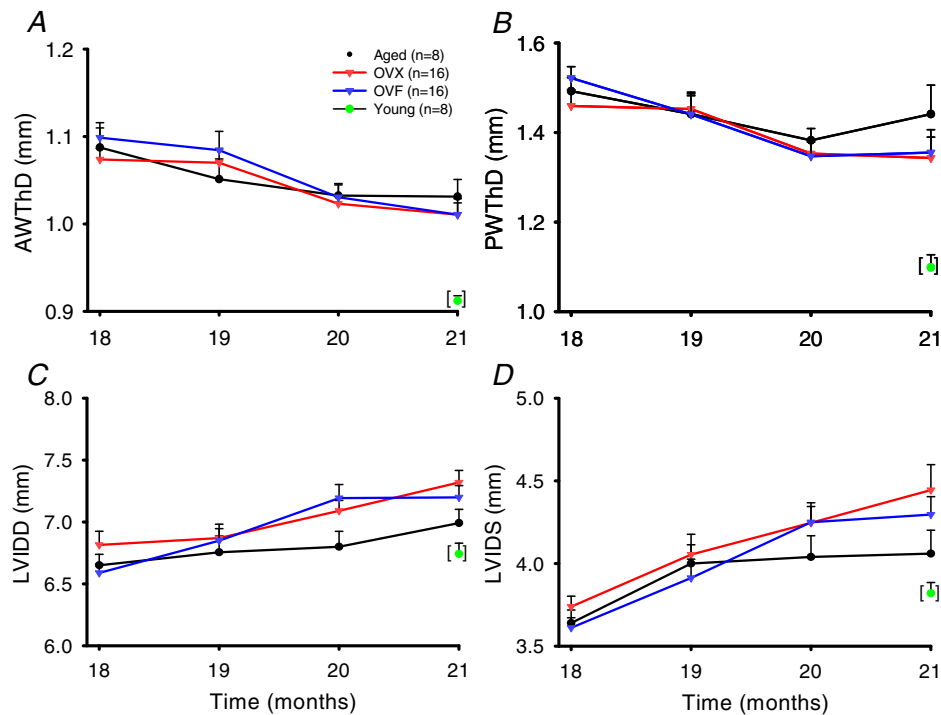
Figure 4. Left ventricular (LV) remodelling as serially tracked by echocardiography
Young group single time-point data included as reference. *A*, anterior wall thickness in diastole (AWThD). *B*, posterior wall thickness in diastole (PWThD). *C*, LV internal diameter diastole (LVIDD). *D*, LV internal diameter in systole (LVIDS). Values are mean ± SEM. For panels *A–D*, *P* < 0.001 for time-dependent changes in all groups. OVF, ovariectomized + fructose; OVX, ovariectomized. [Colour figure can be viewed at wileyonlinelibrary.com]

Table 2. Arterial and left ventricular (LV) haemodynamics by conductance catheter of young (Y), aged (A), ovariectomized (OVX) and ovariectomized + fructose (OVF) Fischer 344 female rats

Parameter	Group Y (n = 8)	A (n = 8)	OVX (n = 16)	OVF (n = 16)	P	Two-way ANOVA A vs. Y	OVX vs. Y	OVF vs. Y	OVX vs. A	OVF vs. A	OVF vs. OVX
SAC BW (g)	178.0 ± 2.1	238.3 ± 8.6	253.4 ± 5.4	290.8 ± 4.9	<0.001	<0.001	<0.001	<0.001	0.083	<0.001	<0.001
BSA (cm^2)	311.0 ± 2.4	377.4 ± 8.9	393.4 ± 5.7	431.3 ± 4.9	<0.001	<0.001	<0.001	<0.001	0.077	<0.001	<0.001
SW (mmHg ml)	157.2 ± 12.0	214.1 ± 18.6	143.4 ± 8.7	146.3 ± 10.8	0.001	0.031	0.824	0.789	0.001	0.002	0.842
CO (ml/min)	63.5 ± 6.3	63.5 ± 6.3	44.8 ± 2.4	46.3 ± 2.8	< 0.001	0.899	<0.001	0.002	0.002	0.004	0.723
Cardiac index	0.212 ± 0.010	0.169 ± 0.017	0.114 ± 0.006	0.108 ± 0.007	< 0.001	0.015	< 0.001	<0.001	<0.001	<0.001	0.579
SV (μl)	194.8 ± 9.6	214.9 ± 29.3	167.2 ± 7.9	161.8 ± 8.8	0.031	0.605	0.404	0.323	0.051	0.049	0.730
SV index	0.627 ± 0.032	0.573 ± 0.080	0.427 ± 0.022	0.376 ± 0.022	<0.001	0.378	0.002	<0.001	0.024	0.002	0.426
V_{max} (μl)	386.6 ± 28.4	373.2 ± 29.1	339.0 ± 17.8	351.5 ± 31.9	0.667	NA	NA	NA	NA	NA	NA
V_{min} (μl)	191.8 ± 24.7	158.3 ± 27.8	171.8 ± 14.8	183.4 ± 30.3	0.870	NA	NA	NA	NA	NA	NA
V_{es} (μl)	208.1 ± 23.8	176.1 ± 27.4	198.5 ± 16.2	213.1 ± 32.5	0.830	NA	NA	NA	NA	NA	NA
V_{ed} (μl)	347.6 ± 31.9	350.6 ± 31.9	312.8 ± 17.1	318.9 ± 32.1	0.746	NA	NA	NA	NA	NA	NA
EDV index	1.121 ± 0.107	0.936 ± 0.093	0.800 ± 0.047	0.745 ± 0.078	0.013	0.434	0.040	0.013	0.432	0.361	0.563
P_{max}	114.1 ± 5.2	148.2 ± 11.6	138.0 ± 6.6	142.9 ± 6.1	0.042	0.050	0.133	0.049	0.740	0.636	0.831
P_{dev}	112.8 ± 5.3	146.3 ± 10.8	135.0 ± 6.0	140.8 ± 5.9	0.031	0.044	0.140	0.046	0.631	0.603	0.744
P_{es}	111.5 ± 5.0	144.1 ± 11.0	134.9 ± 6.2	139.6 ± 6.0	0.038	0.047	0.946	0.049	0.813	0.617	0.946
EF%	55.1 ± 4.1	61.4 ± 7.0	53.2 ± 2.6	56.3 ± 5.7	0.747	NA	NA	NA	NA	NA	NA
E_a	0.58 ± 0.03	0.759 ± 0.098	0.867 ± 0.094	0.913 ± 0.065	0.006	ns	<0.05	<0.05	ns	ns	ns
dP/dt_{max}	6645 ± 453	7902 ± 880	6459 ± 367	7001 ± 454	0.282	NA	NA	NA	NA	NA	NA
dP/dt_{min}	−9018 ± 621	−9377 ± 1158	−7746 ± 456	−8112 ± 638	0.192	NA	NA	NA	NA	NA	NA
dV/dt_{max}	8587 ± 516	7607 ± 734	6776 ± 734	6719 ± 438	0.077	NA	NA	NA	NA	NA	NA
dV/dt_{min}	−12937 ± 2451	−13087 ± 1762	−9511 ± 1525	−9189 ± 1192	0.228	NA	NA	NA	NA	NA	NA
Tau	10.0 ± 0.3	12.6 ± 0.9	13.8 ± 0.4	13.4 ± 0.5	<0.001	0.044	<0.001	<0.001	0.441	0.692	0.958
$P_{ao,sys}$	122.1 ± 6.9	180.5 ± 9.2	163.6 ± 7.4	166.7 ± 11.6	0.009	0.010	0.034	0.024	0.604	0.594	0.800
$P_{ao,dia}$	99.9 ± 3.3	115.3 ± 5.6	112.2 ± 3.8	111.6 ± 3.8	0.318	NA	NA	NA	NA	NA	NA
$P_{ao,mean}$	110.4 ± 4.1	142.7 ± 7.4	134.1 ± 5.0	134.1 ± 5.0	0.051	NA	NA	NA	NA	NA	NA
HR	339.0 ± 7.1	302.2 ± 11.3	271.4 ± 11.3	287.9 ± 9.9	0.002	0.220	0.001	0.017	0.193	0.391	0.404
PRSW	64.1 ± 4.5	73.8 ± 7.3	75.2 ± 4.5	74.3 ± 6.8	0.654	NA	NA	NA	NA	NA	NA
ESPVR slope	0.397 ± 0.03	0.617 ± 0.21	0.496 ± 0.101	0.675 ± 0.10	0.179	NA	NA	NA	NA	NA	NA
EDPVR slope	0.042 ± 0.006	0.0311 ± 0.005	0.0573 ± 0.007	0.0410 ± 0.004	0.022	0.484	0.285	0.896	0.030	0.610	0.111
EDVPR inter	−9.749 ± 3.55	−3.87 ± 2.01	−10.01 ± 2.22	−6.602 ± 1.87	0.329	NA	NA	NA	NA	NA	NA

Values are means ± SEM. NA, subgroup analysis not applicable. BSA, body surface area; CO, cardiac output; dP/dt_{max}, maximal rate of LV pressure rise over time; dP/dt_{min}, minimum rate of LV pressure decrease over time; E_a, arterial elastance; EDPVR, end-diastolic pressure–volume relationship slope; EDPVR inter, end-diastolic pressure volume relationship intercept; EDV, end-diastolic volume; EF, ejection fraction; ESPVR, end-systolic pressure–volume relationship slope; HR, heart rate; $P_{ao,dia}$, aortic diastolic pressure; $P_{ao,mean}$, mean aortic pressure; $P_{ao,sys}$, aortic systolic pressure; P_{dev}, LV developed pressure; P_{es}, end-systolic pressure; P_{max}, maximal LV pressure; PRSW, preload recruitable stroke work; SAC BW, terminal body weight; SV, stroke volume; SW, stroke work; Tau, isovolumic relaxation time constant; V_{max}, LV maximal volume; V_{ed}, end-diastolic volume; V_{es}, end-systolic volume; V_{min}, LV minimal volume.

50% (observed in control 4-month-old animals) to 40% and was restored by oestradiol supplementation. These changes were associated with the activation of regulators of inflammation in isolated myocytes, which were also suppressed by oestradiol. In a recent study by Alencar *et al.* (2017), the influence of ageing and oestrogen depletion on LV structure/function was examined in hybrid female F344BN rats. A subgroup of animals at 18 months of age underwent an ovariectomy for 2 months and relevant endpoints were examined. In their study, ovariectomy did not alter blood pressure, systolic function or lead to the development of hypertrophy or additional interstitial fibrosis beyond that noted for ageing. Significant alterations were only noted in LV relaxation and increases in filling pressure. Our echocardiography remodelling and systolic function data essentially replicate their results pertaining to the apparent lack of 'added'

effects derived from ovariectomy. However, our use of a high-fidelity conductance catheter allowed us to provide evidence for a rather large (∼30%) significant loss in stroke volume index, cardiac output index and increased arterial elastance in the presence of preserved EF in OVX rats that was not detected by echocardiography. *Ex vivo* LV passive PV curves did not demonstrate global changes in passive properties. However, OVX group EDPVR slopes were modestly higher *vs.* ageing. Conductance catheter results also replicated the increased in Tau noted in intact aged rats. Ovariectomy did not lead to further increases in collagen area fraction but did appear to uniquely influence the distribution of myocardial fibrosis towards the endocardium (*vs.* epicardium). Interestingly, papillary fibrosis was notably increased in OVX animals *vs.* ageing alone and may have important implications for disease development in the presence of mitral valve dysfunction.

In an attempt to incorporate excess body weight into our animal model, we utilized 10% fructose in water in OVX rats. As expected, ageing over 3 months led to a modest increase in body weight of ~6% while OVX yielded ~8% and OVF ~19%. However, none of the *in vivo, ex vivo* or histological endpoints showed greater differences between the OVF *vs.* the OVX groups. Thus, using this model, excess weight did not lead to greater, adverse changes in LV structure/function. A limitation of the approach used is that a blood-based metabolic profiling of these animals groups was not pursued.

As noted above, 'typical' female patients with HFpEF are older and suffer from hypertension and excess weight. Their hearts typically show minimal degrees of LV remodelling with fibrosis, and increases in active relaxation times while preserving EF. Reductions in CO typically become apparent upon physical exertion. The aged, female animal model implemented in this study recapitulates many of these features, and highlights an important role for ovarian hormones in the maintenance of CO and possibly in the redistribution of excess interstitial cardiac collagens across the LV wall, and development of papillary fibrosis. These changes would likely be accentuated if animals were allowed to survive for a longer period of time and could lead to the development of a detectable HF phenotype. Furthermore, changes in the quality of collagen fibres would also need to be determined as, for example, the crosslinking of fibres can alter their mechanical properties. Surprisingly, the development of interstitial fibrosis as a function of ageing (about double *vs.* young) did not alter the mechanical properties of the LV in a uniform manner. However, an increase in Tau suggests impaired 'active' relaxation, likely related to alterations in calcium handling, which has been reported in other studies (Yang *et al.* 2017). The loss in stroke volume (and consequently in CO) in OVX does indicate that oestrogen depletion can contribute to impaired pump function. These data suggest that the use of invasive methods may
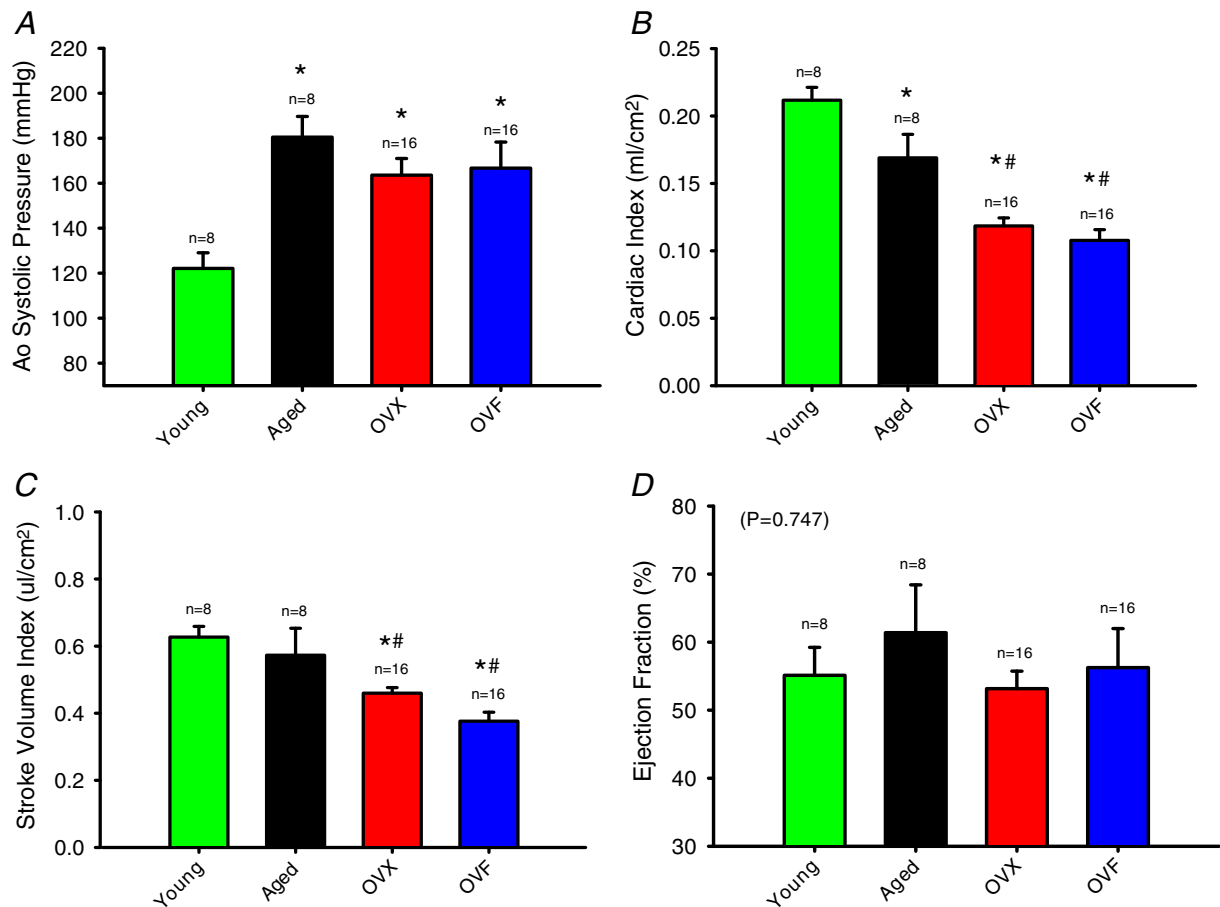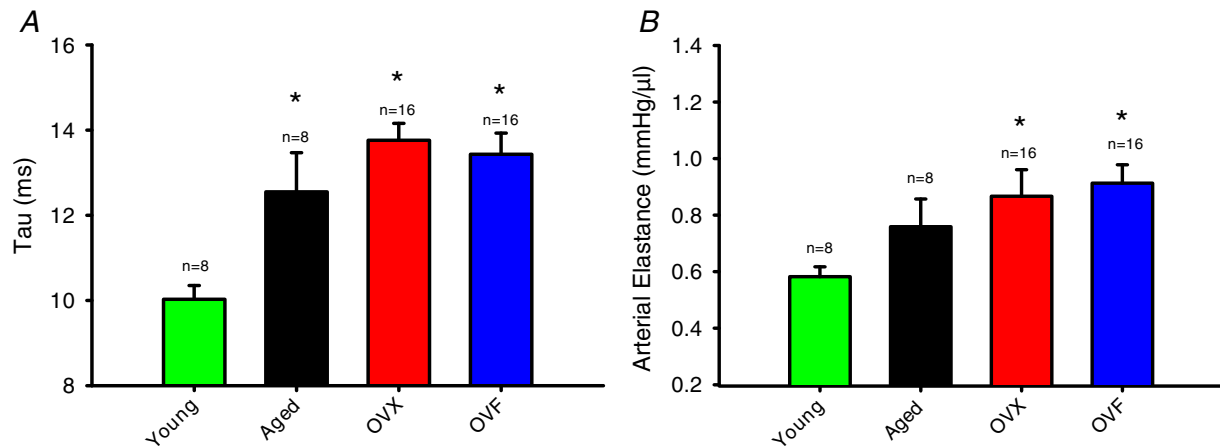

Figure 5. Haemodynamic values derived from arterial and left ventricular (LV) conductance catheter measurements during the terminal study

A, systolic aortic pressure ($P < 0.05$ aged, OVX and OVF *vs.* young). *B*, cardiac index (*$P < 0.05$, aged, OVX and OVF *vs.* young; and #$P < 0.05$, OVX and OVF *vs.* aged). *C*, stroke volume index ($P < 0.05$ OVX and OVF *vs.* young, and #$P < 0.05$, OVX and OVF *vs.* aged). *D*, ejection fraction. Values are means ± SEM. OVF, ovariectomized + fructose; OVX, ovariectomized. [Colour figure can be viewed at wileyonlinelibrary.com]

be required to accurately detect HFpEF in animal models. It is worth noting that all active functional measurements in the current studies were done with the animal in a 'resting' state. The true unmasking of the effect that specific interventions have in aged models may require the use of 'stress' interventions such as a dobutamine infusion during the acquisition of LV haemodynamics. This modality of testing would be equivalent to that done in HFpEF patients when stressed by exercise or heart rate stimulation to truly unmask the degree of LV dysfunction.

Figure 6. Hemodynamic values derived from arterial and left ventricular (LV) conductance catheter measurements during the terminal study
A, LV isovolumic relaxation time constant (Tau) ($P < 0.05$ aged, OVX and OVF *vs.* young). *B*, arterial elastance ($P < 0.05$ OVX and OVF *vs.* young). Values are means $\pm$ SEM. OVF, ovariectomized + fructose; OVX, ovariectomized. [Colour figure can be viewed at wileyonlinelibrary.com]
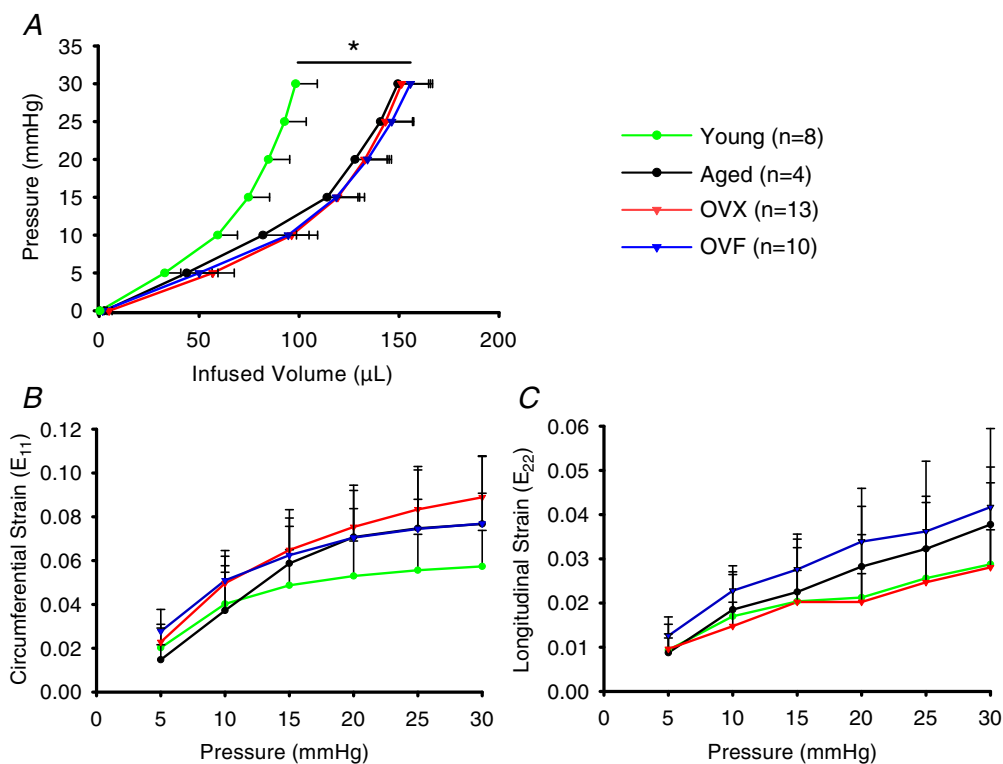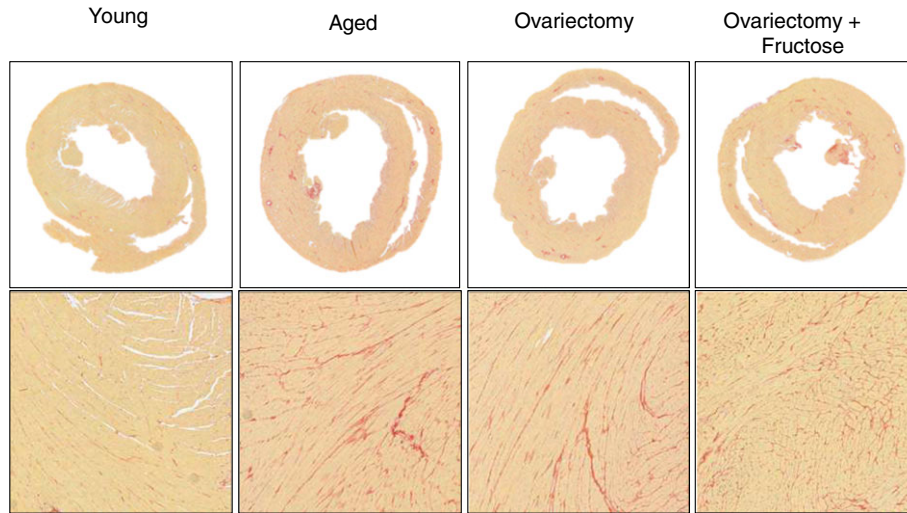

Figure 7. *Ex vivo* analysis of left ventricular (LV) mechanics
*A*, passive LV pressure–volume (PV) curves for all groups at 21 months of age ($P < 0.001$ aged, OVX and OVF *vs.* young). *B* and *C*, two-dimensional circumferential (E_{11}) and longitudinal (E_{22}) LV epicardial strains at incremental LV pressures. *$P < 0.001$, OVX *vs.* young. Values are means $\pm$ SEM. OVF, ovariectomized + fructose; OVX, ovariectomized. [Colour figure can be viewed at wileyonlinelibrary.com]

As the pathophysiology of HFpEF remains unclear, the identification and modelling of early stages of the disease is critical to its understanding. It is difficult to envision such measurements in a patient population at risk since the disease is likely to progress slowly over time. Thus, the need to develop and implement animal models that incorporate recognized risk factors and 'mimic' early stages of the pathology allow for the evaluation of therapeutic strategies targeting those elements identified as critical to its evolution. Thus, the use of aged female rats undergoing ovariectomy may allow investigators to further examine the role that oestrogen depletion plays in

Figure 8. Composite of representative panels for left ventricular collagen as derived from Sirius Red staining
[Colour figure can be viewed at wileyonlinelibrary.com]
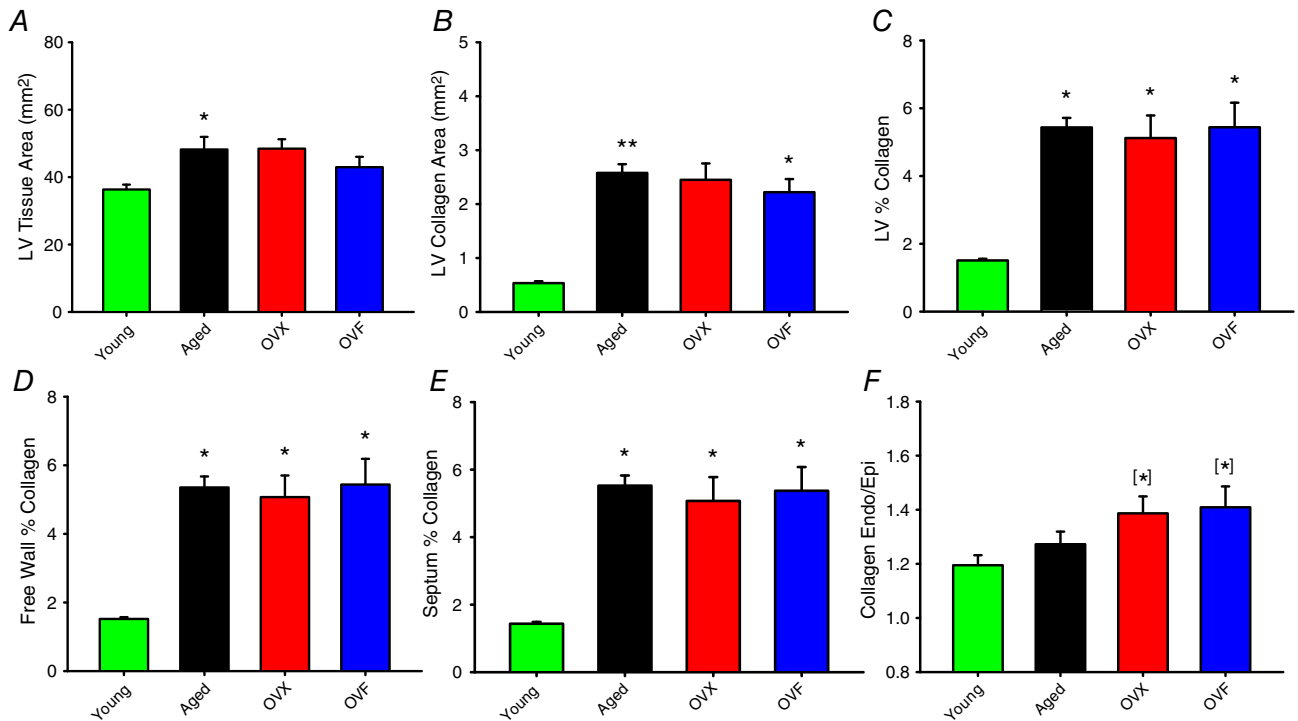
Figure 9. Morphometric and histological analysis of left ventricular (LV) tissue sections
A, LV tissue area; *B*, LV collagen area; *C*, LV % collagen (collagen/LV area); *D*, free wall percentage collagen; *E*, septum percentage collagen; *F*, endocardium/epicardium collagen ratio. Values are means ± SEM. $*P < 0.05$ *vs.* young, ANOVA. [*]$P < 0.05$ *vs.* young, unpaired *t* test. Endo: endocardium; Epi: epicardium; OVF, ovariectomized + fructose; OVX, ovariectomized. [Colour figure can be viewed at wileyonlinelibrary.com]

the early stages of HFpEF development, as well as to test for pharmacological interventions that may modify this process.

References

Alencar AK, da Silva JS, Lin M, Silva AM, Sun X, Ferrario CM, Cheng C, Sudo RT, Zapata-Sudo G, Wang H & Groban L (2017). Effect of age, estrogen status, and late-life GPER activation on cardiac structure and function in the Fischer344×Brown Norway female rat. *J Gerontol A Biol Sci Med Sci* **72**, 152–162.

Barandiarán Aizpurua A, Schroen B, van Bilsen M & van Empel VPM (2019). Targeted HFpEF therapy based on matchmaking of human and animal models. *Am J Physiol Circ Physiol* **315**, H1670–H1683.

Barasch E, Gottdiener JS, Aurigemma G, Kitzman DW, Han J, Kop WJ & Tracy RP (2009). Association between elevated fibrosis markers and heart failure in the elderly: the cardiovascular health study. *Circ Heart Fail* **2**, 303–310.

Bhuiyan MS, Shioda N & Fukunaga K (2007). Ovariectomy augments pressure overload-induced hypertrophy associated with changes in Akt and nitric oxide synthase signaling pathways in female rats. *Am J Physiol Endocrinol Metab* **293**, E1606–E1614.

Boluyt MO (2004). Echocardiographic assessment of age-associated changes in systolic and diastolic function of the female F344 rat heart. *J Appl Physiol* **96**, 822–828.

Borlaug BA (2014). The pathophysiology of heart failure with preserved ejection fraction. *Nat Rev Cardiol* **11**, 507–515.

Borlaug BA (2016). Is HFpEF one disease or many? *J Am Coll Cardiol* **67**, 671–673.

Conceição G, Heinonen I, Lourenço AP, Duncker DJ & Falcão-Pires I (2016). Animal models of heart failure with preserved ejection fraction. *Netherlands Heart J* **24**, 275–286.

Douglas PS, Katz SE, Weinberg EO, Chen MH, Bishop SP & Lorell BH (1998). Hypertrophic remodeling: Gender differences in the early response to left ventricular pressure overload. *J Am Coll Cardiol* **32**, 1118–1125.

Eaton CB, Pettinger M, Rossouw J, Martin LW, Foraker R, Quddus A, Liu S, Wampler NS, Hank Wu W-C, Manson JE, Margolis K, Johnson KC, Allison M, Corbie-Smith G, Rosamond W, Breathett K & Klein L (2016). Risk factors for incident hospitalized heart failure with preserved versus reduced ejection fraction in a multiracial cohort of postmenopausal women. *Circ Heart Fail* **9**, e002883.

Fannin J, Rice KM, Thulluri S, Dornon L, Arvapalli RK, Wehner P & Blough ER (2014). Age-associated alterations of cardiac structure and function in the female F344xBN rat heart. *Age (Omaha)* **36**, 9684.

Forman DE, Cittadini A, Azhar G, Douglas PS & Wei JY (1997). Cardiac morphology and function in senescent rats: Gender-related differences. *J Am Coll Cardiol* **30**, 1872–1877.

Hacker TA (2005). Age-related changes in cardiac structure and function in Fischer 344 × Brown Norway hybrid rats. *AJP Hear Circ Physiol* **290**, H304–H311.

Knowlton AA & Lee AR (2012). Estrogen and the cardiovascular system. *Pharmacol Ther* **135**, 54–70.

Lam CSP, Donal E, Kraigher-Krainer E & Vasan RS (2011). Epidemiology and clinical course of heart failure with preserved ejection fraction. *Eur J Heart Fail* **13**, 18–28.

Liu CY, Liu YC, Wu C, Armstrong A, Volpe GJ, van der Geest RJ, Liu Y, Hundley WG, Gomes AS, Liu S, Nacif M, Bluemke DA & Lima JAC (2014). Evaluation of age-related interstitial myocardial fibrosis with cardiac magnetic resonance contrast-enhanced T1 mapping: MESA (Multi-Ethnic Study of Atherosclerosis). **62**, 1280–1287.

Omar AMS, Bansal M & Sengupta PP (2016). Advances in echocardiographic imaging in heart failure with reduced and preserved ejection fraction. *Circ Res* **119**, 357–374.

Omens JH, MacKenna DA & McCulloch AD (1993). Measurement of strain and analysis of stress in resting rat left ventricular myocardium. *J Biomech* **26**, 665–676.

Omens JH, Milkes DE & Covell JW (1995). Effects of pressure overload on the passive mechanics of the rat left ventricle. *Ann Biomed Eng* **23**, 152–163.

Owan TE, Hodge DO, Herges RM, Jacobsen SJ, Roger VL & Redfield MM (2006). Trends in prevalence and outcome of heart failure with preserved ejection fraction. *N Engl J Med* **355**, 251–259.

Pacher P, Mabley JG, Liaudet L, Evgenov O V, Marton A, Haskó G, Kollai M & Szabó C (2004). Left ventricular pressure-volume relationship in a rat model of advanced aging-associated heart failure. *Am J Physiol Heart Circ Physiol* **287**, H2132–H2137.

Pacher P, Nagayama T, Mukhopadhyay P, Bátkai S & Kass DA (2008). Measurement of cardiac function using pressure-volume conductance catheter technique in mice and rats. *Nat Protoc* **3**, 1422–1434.

Sohrabji F (2005). Estrogen: A neuroprotective or proinflammatory hormone? Emerging evidence from reproductive aging models. *Ann N Y Acad Sci* **1052**, 75–90.

Stice JP, Chen L, Kim SC, Jung JS, Tran AL, Liu TT & Knowlton AA (2011). 17β-Estradiol, aging, inflammation, and the stress response in the female heart. *Endocrinology* **152**, 1589–1598.

Stout Steele M & Bennett RA (2011). Clinical technique: Dorsal ovariectomy in rodents. *J Exot Pet Med* **20**, 222–226.

Takahashi TA & Johnson KM (2015). Menopause. *Med Clin North Am* **99**, 521–534.

Valero-Muñoz M, Backman W & Sam F (2017). Murine models of heart failure with preserved ejection fraction: A "fishing expedition." *JACC Basic to Transl Sci* **2**, 770–789.

Yang H-Y, Firth JM, Francis AJ, Alvarez-Laviada A & MacLeod KT (2017). The effect of ovariectomy on intracellular calcium (Ca^{2+}) regulation in guinea pig cardiomyocytes. *Am J Physiol Hear Circ Physiol* **313**, H1031–H1043.

Zhao Z, Wang H, Jessup JA, Lindsey SH, Chappell MC & Groban L (2014). Role of estrogen in diastolic dysfunction. *AJP Hear Circ Physiol* **306**, H628–H640.

Additional information

Competing interests

Author contributions

MB, BI, RG, GC, JO and FV conceptualized and designed the work. All authors contributed to acquisition, analysis, interpretation, and drafting. Experiments were performed at UCSD. All authors have read and approved the final version of this manuscript and agree to be accountable for all aspects of the work in ensuring that questions related to the accuracy or integrity of any part of the work are appropriately investigated and resolved. All persons designated as authors qualify for authorship, and all those who qualify for authorship are listed.